Identification of a Novel Locus Associated with Congenital Recessive Ichthyosis on 12p11.2–q13

Mordechai Mizrachi-Koren,*† Dan Geiger,‡ Margarita Indelman,* Ora Bitterman-Deutsch,§ Reuven Bergman,*¶ and Eli Sprecher*¶

*Laboratory of Molecular Dermatology, Department of Dermatology, Rambam Medical Center; †Biotechnology Interdisciplinary Unit and ‡Computer Science Department, Israel Institute of Technology, Haifa, Israel; §Dermatology Unit, Western Galile Hospital, Naharya, Israel; ¶Bruce Rappaport Faculty of Medicine, Technion, Israel Institute of Technology, Haifa, Israel

Congenital recessive ichthyoses represent a vast and markedly heterogeneous group of diseases that have been mapped to at least seven distinct chromosomal loci. In this study, we ascertained two consanguineous families presenting with congenital ichthyosis. Using homozygosity mapping, we identified a 6.5 cM homozygous region on 12p11.2–q13 shared by all affected individuals. Multipoint logarithm of odds ratio (LOD) score analysis placed the new locus between markers D12S345 and D12S390 with a maximum LOD score of 4.79 at marker CH12SSR13. This region harbors *PPHLN1*, encoding periphilin 1, a protein involved in the cornification process. No deleterious mutations were identified within the coding region of this gene, suggesting the existence of another gene associated with epidermal differentiation on 12p11.2–q13.

Key words: ichthyosis/cornification/genetic/mapping/homozygosity/periphilin
J Invest Dermatol 125:456–462, 2005

The recent years have witnessed spectacular advances in our understanding of disorders of cornification (Irvine and Paller, 2002). Mutations in genes encoding numerous proteins involved in the process of keratinization have been shown to cause a spectrum of inherited skin disorders, among which the ichthyoses, a clinically and genetically heterogeneous group of genodermatoses, rank first in severity and prevalence (Irvine and Paller, 2002). These disorders are often associated with defective skin barrier function, which can result in fluid and electrolyte imbalance, as well as life-threatening infections.

Ichthyoses are usually classified based on inheritance pattern, morphology and distribution of the scales, histological findings, and associated features. Congenital recessive ichthyoses (CRI) can be divided into non-syndromic and syndromic forms. The latter group includes numerous complex disorders such as Sjogren–Larsson syndrome (MIM270200) resulting from mutations in the fatty aldehyde dehydrogenase gene (De Laurenzi *et al*, 1996), Chanarin–Dorfman syndrome (MIM275630), a neutral lipid storage disease caused by mutations in CGI-58 (Lefevre *et al*, 2001), and Netherton syndrome (MIM256500) characterized by congenital ichthyosis, elevated levels of IgE, and hair structural anomalies, which results from mutations in SPINK5, encoding a serine protease inhibitor (Chavanas *et al*, 2000). The clinical spectrum of non-syndromic CRI includes severe, classic lamellar ichthyosis (LI1 MIM242300, LI2 MIM601277, LI3 MIM604777, LI5 MIM606545) characterized by collodion membrane presentation (neonates born with a shiny and transparent cover that dries to thick, hard skin, then cracks, and fissures), development of large, plate-like scales, ectropion (turning out of eyelids), eclabium (turning out of the lips) but no erythema (Williams and Elias, 1985). A second distinct subtype of CRI is congenital ichthyosiform erythroderma (CIE; MIM242100). The presence of an intense, generalized erythema and fine, white scales define this disease (Akiyama *et al*, 2003). Patients may also manifest as collodion baby, and may have decreased sweating with severe heat intolerance. About 30% of all patients with CRI have mutations in the gene TGM1 on chromosome 14q (Russel *et al*, 1995; Laiho *et al*, 1997). This gene encodes the enzyme transglutaminase-1, which catalyzes the transamidation of glutamine residues during the cross-linking of the cornified envelope proteins (Ishida-Yamamoto and Izuka, 2002). CRI has also been shown to be caused by mutations in genes encoding lipoxygenase-3 and 12(R)-lipoxygenase (ALOXE3, ALOX12B) on 17p13.1 (Jobard *et al*, 2002), the ATP-binding cassette (ABC)A12 transporter on 2q (Lefevre *et al*, 2003), and ichthyin on 5q33 (Lefevre, 2004). Other CRI cases have been mapped to 12q13 and 19p13.1–13.2 (Fischer *et al*, 2000; Virolainene *et al*; 2000; Hatsell *et al*, 2003), but the causative genes associated with these loci remain to be uncovered. Moreover, further, so far unknown loci for CRI must exist (Krebsova *et al*, 2001) demonstrating extensive genetic heterogeneity in CRI.

Although no formal epidemiological study of recessive ichthyoses has been performed in the Middle East, they are estimated to be extremely frequent in this region because of a high rate of consanguineous unions (Zlotogora, 1997). In

Abbreviations: ABC, ATP-binding cassette; CRI, congenital recessive ichthyoses; LOD, logarithm of odds ratio

this study, we mapped CRI to 12p11.2–q13 in two Israeli consanguineous families.

Results

Clinical findings We ascertained two Israeli families of Arab Moslem origin comprising 14 individuals, including five patients. In both families, parents were first-degree cousins. All five patients were born with normal-looking skin. No collodion membrane was noticed at birth. A few days after birth, fine whitish scales appeared.

The three patients in family 1 developed typical CIE features during childhood including severe erythroderma associated with generalized fine scaling. The erythroderma partly receded with age, but larger scales appeared and persisted through the years (Fig 1*a*). Palmoplantar keratoderma manifested in all three patients with skin thickening and fissuring (Fig 1*b*). A skin biopsy revealed epidermal compact hyperkeratosis, hypergranulosis, acanthosis, and papillomatosis. Over the years, the patients required repeated antifungal and antibiotic treatment courses because of tinea pedis, onychomycosis, and recalcitrant malodorous secondary bacterial infections. Patients 63 and 64 in family 1 received acitretin (50 mg per d) at the age of 35 and 30 y, respectively, for prolonged periods (1–2 y) with marked improvement.

In contrast with the early features of CIE manifested by family 1 patients, the two affected individuals of family 2 displayed only mild fine generalized scaling with minimal palmoplantar skin thickening (Fig 1*c*). They were treated satisfactorily with skin moisturizers and emollients only.

In both families, growth and psychomotor development had been normal. No other diseases or abnormal laboratory findings were reported.

Identification of a new locus associated with CRI In both families, we initially ruled out linkage to seven known CRI-associated loci on 2q33–p35, 3p21, 12q11–q13, 14q11.2, 17p13.2–13.1, 19p12–q12, 19p13.2–13.1 (not shown). Based upon the fact that the families were consanguineous, we assumed the existence in each family of a homozygous causative mutation. Using a panel of fluorescently labeled markers, we genotyped the three patients of family 1 at 304 microsatellite loci, and scrutinized our results for regions of homozygosity shared by all three affected individuals. We identified such a region between markers D12S85 and D12S345 (not shown).

Because of the very low numbers of informative microsatellite markers available in this region in public databases, we characterized 15 novel markers within the suspected disease interval, six of which were found to be informative in our two families (Table I). Using these and five additional markers derived from the NCBI Mapviewer database (http://www.ncbi.nlm.nih.gov/mapview/map_search.cgi?taxid=9606) and spanning 19.9 cM on 12p11.2–q13, we genotyped all members of families 1 and 2. Multipoint logarithm of odds ratio (LOD) score analysis using the Superlink software for eight markers placed the new CRI-associated locus between markers D12S345 and D12S390 with a maximum LOD score of 4.79 at marker CH12SSR13 (Fig 2). Multipoint LOD score analysis performed separately for each of the two families revealed a positive LOD score of 2.88 for family 1 and 1.91 for family 2. Similar results were obtained using the HOMOZ software, which generated a maximum combined LOD score of 4.05 at marker CH12SSR13.

We established parsimonious haplotypes for each individual (Fig 3). Haplotype analysis revealed critical recombination events in individuals 68 and 65 at markers D12S1648 and D12S85, respectively, therefore defining the upper and lower boundaries of the disease interval in this family.

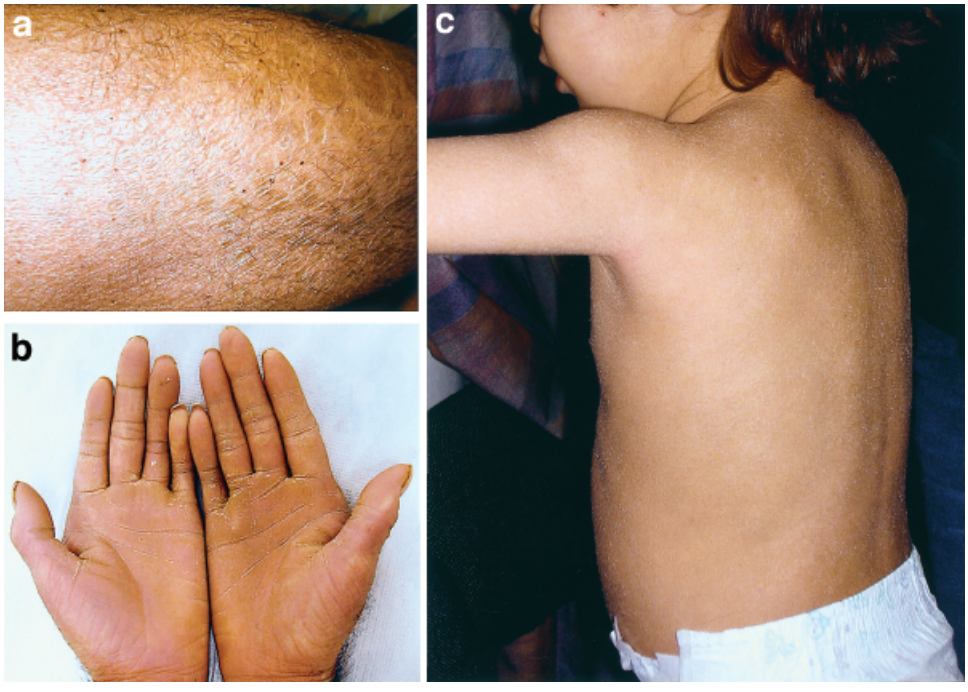

Figure 1
Clinical features. (*a*) Large lamellar scales over the left thigh of patient 64. (*b*) Thickening of the palmar skin in patient 63. (*c*) Fine whitish scales cover the skin of patient 93.

Table I. Nucleotide sequences of primers used for genotyping microsatellite loci

Name	Forward primer	Reverse primer	Product size (bp)	Annealing temperature (°C)
D12S1294	CCAGTTTAGACACCCAGGAT	ATATTTCAGAACCGCAGCAG	168–204	55
D12S1301	ACACAGATGTGCATCTATCTCG	TATTGGACAGTAAAGAAACCTGC	100–120	55
D12S297	GTTTGGTATTGGAGTTTTCAG	AAATCATCAGTGGAGTTAGCA	205–269	55
D12S1586	CTGCACCAAGGCAGGAAC	AATTCCAGGCCCACACTTT	151–175	60
D12S1713	GCTATTTGGGAGGCCAGTTG	TCCCTCTGGGTAGAATGTTTTTG	149–183	60
D12S368	ACCCCTAGAGGCCTAGAAAT	AGCTGTCCAAGAGGAAGTCT	127–131	60
D12S390	AGCCTCCCAGATTACATCAG	GAGATATCCTTTCGGTTATACACA	148–162	57
D12S1687	GCCAGCTTCCAGCTAGG	GAAATGCTGATATTCAATTTAGGAC	163–169	57
D12S1456	CTCACAGATTCAAGAATCTAAGGAA	CTTAATGTGCAAGATTTTCTCTGTC	148–152	55
D12S2010	AAACAAACATACATTGTTTCATTGA	GTGTAATGGAAGACCTTTGAGAA	148–152	55
D12S1337	ATTCCAAGGACTACTCAGG	TGTGGACTAAATATCTGTCAT	253–255	55
D12S1704	CATGATACCCAAAACGATGACATAG	CACCAGCAAGGATACCTACTGTAA	116–124	55
D12S87	CACTAGGTGATGCTGGACAT	CTGCACAAACACTTGAAACA	142–168	55
D12S1648	TGGGTGCTTTCACACACA	GGAGATGAGGAGCCTTGC	90–144	55
D12S1584	CGTAGAATATGCACCTAATTTTAAT	CCAGGGAAACATAGTGAGAA	159–179	55
D12S1621	AGCTCTCTACACCAATGTAGCATAT	AAGGGATTTCATAAGATACTGAATG	175–201	55
D12S1048	GGTCTGCTTAGGTCCCTTTT	AAGGAACCAAGGAGTGGAAG	209–229	55
D12S291	GTCTCTTGTACATCATGGTG	ACTCACTTTGCTTACAGCTTT	149–151	55
D12S1668	GAATTGCTTGACCCCG	GCCACTATCCTGACGACTAA	236–260	55
D12S1473	CTCACTCAAACTAATGCCCA	TAGAGAAGTTACGATATAAAGCTC	213	55
D12S1334	AGCACTCCATCCTGGGTGA	CATCCTCCTGCCTTAGCCT	125	55
D12S1372	TTCAGATGGGTGATTTAAGTGAG	AAACTATGTTAACAGAGCAGT	148	55
D12S1824	GTTCTCTTTTCCCTCCCTCCT	CTGAGAGGAAACTACAGTCCAGC	206	55
CH12SSR1[a]	GTAAAGTAATCTTCCAGAT	AGTTTGAAAGCAATCTCTAGAG	285	57
CH12SSR2[a]	GAGAGCCAGCTTTAATAAACATC	GTTATTATTTACATGTCCCAGAGC	274	5
CH12SSR3[a]	GGTTGCTGGTAACTGCAACTTTC	CCACTGCACTCCAGCCTGGCAGCC	228	5
CH12SSR4[a]	GCATTCTCCATCCTCCACGCGCAATC	GTCATGAAAGTCCTGAAGTAGTGAC	340	57
CH12SSR5[a]	GTCTTTCAGTCAATACATTTAGTTC	CACACTGCAAAGTTCATTGCTTC	306	55
CH12SSR6[a]	GCCTGAAAGATAGCGGCGGC	GAATTGGTATAATAGGATGTTTCATC	198	55
CH12SSR7[a]	GCAGCCTTCACCTCTGAGCTG	CCAGAGGCATTCTGGAGAGCAAC	242	55
CH12SSR8[a]	GGAAGATAGAATGGAAAACCTG	GAGACCTCTCTTCAGCCAC	216	55
CH12SSR9[a]	GTTCAGCCAATGTATTTCTCAGTTC	CAGGTTCAGGCCACTGCACTCCAGT	186	60
CH12SSR10[a]	GCTACCTGTGAATTTGTCCTAAC	GCTGGGGTTCAAGGTTCTCCAATTAC	194	55
CH12SSR11[a]	GTTAGGAACTCAGCGACTGAAGC	CAGCAGCCATCATACAACC	252	55
CH12SSR12[a]	GAATTTAGAAACATTTCTTATTGGC	CTCAGGTATTTCACCTGCCTTGGCC	271	55
CH12SSR13[a]	GATGTAGTGCTGACAAGCCAGAG	GCAATGTAAGGTGTAGATAAGC	348	57
CH12SSR14[a]	GAGGAACTAGTATTTACCAGTC	GCCTTCTTTTCACAGGCTACTTTC	165	57
CH12SSR15[a]	GTTATGGTTGCTAAAATTATTTGAG	GGTCTTAATTTACCAGTCTACTC	257	60

[a]Novel microsatellite markers were deposited in GenBank under accession numbers BV210260 (CH12SSR1), BV210261 (CH12SSR4), BV10262 (CH12SSR9), BV10263 (CH12SSR13), BV10264 (CH12SSR14), BV210265 (CH12SSR15). All markers are dinucleotide repeats except for CH12SSR13, which is a tetranucleotide repeat.

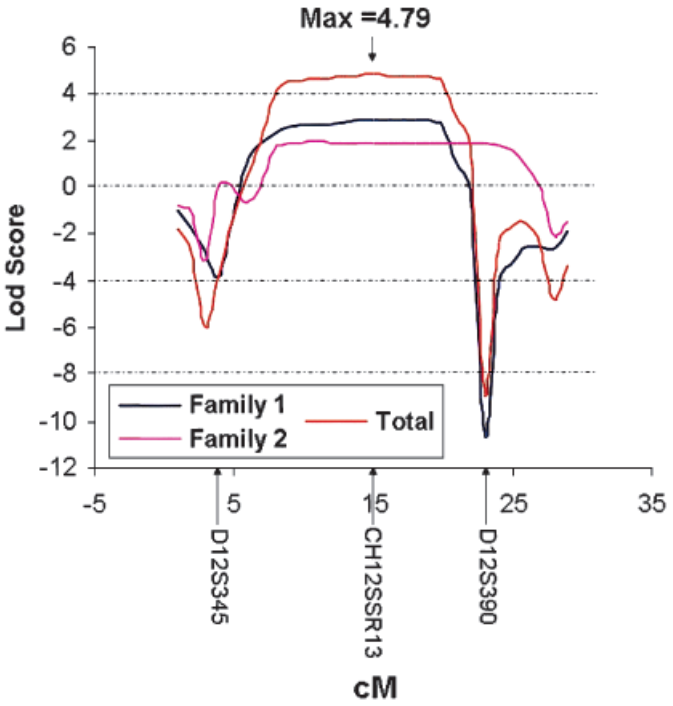

Figure 2
Multipoint linkage map across the candidate region on 12p11.2–q13 for the two congenital recessive ichthyoses (CRI) families. Maximal combined lode score is obtained for marker CH12SSR13.

Haplotype analysis in family 2 did not help reduce the interval defined by analysis of family 1, since patients in this family were found to share a homozygous haplotype spanning more than 12 cM. The disease-associated region was found to span less than 6.5 cM. This novel locus is located 5 cM centromeric to the locus previously described by Hatsell *et al* (2003).

Candidate gene analysis Using MapViewer (http://www.ncbi.nlm.nih.gov/mapview/), we ascertained the disease interval. A total of 73 genes were identified within this interval (Fig 4). Forty-seven genes are predicted open reading frames of unknown significance. Twenty-six genes have a known function, among which *PPHLN1*, encoding periphilin1, was considered as a prime candidate. Periphilin 1 is one of several proteins that become sequentially incorporated into the cornified cell envelope during the terminal differentiation of keratinocytes at the outer layers of the epidermis (Kazerounian and Aho, 2003).

We developed primer pairs and established PCR conditions to amplify all exons and exon–intron boundaries of the *PPHLN1* gene (Table II). Genomic DNA obtained from one affected child of family 1 and one affected child from family 2 was assessed for sequence alterations in *PPHLN1*. No pathogenic mutation was found in *PPHLN1* in both patients. To examine the possibility that a mutation located within a non-coding region may influence the gene expression, we extracted RNA from a skin biopsy obtained from patient 63 of family 1. We used RT-PCR to assess the gene expression in patient *versus* control skin. No evidence of reduced *PPHLN1* expression in the patient's skin was observed in comparison with normal skin (not shown). These results suggest the existence of a gene associated with CRI on 12p11.2–q13 that is distinct from *PPHLN1*.

Discussion

In this study, we describe a novel chromosomal locus linked to CRI in two consanguineous families. This locus is the eight CRI-associated locus reported in recent years and adds to the steadily growing body of evidence pointing to extensive genetic heterogeneity in recessive ichthyoses (Krebsova *et al*, 2001; DiGiovanna *et al*, 2003).

The 12p11.2–q13 locus was found to be centromeric to a neighboring locus on 12q11–q13 previously described in another consanguineous Israeli family of Bedouin origin (Hatsell *et al*, 2003). Of note is the fact that in this study (Hatsell *et al*, 2003), the mother of the family was homozygous for a series of markers encompassing the disease-critical interval, so that a recombination event within this region could not be totally excluded. Interestingly, none of nine other consanguineous CRI Israeli families that we recently assessed mapped to the 12q11–q13 or to the 12p11.2–q13 loci (not shown). These families displayed a more severe phenotype than the two families described in the present report.

Because of their relatively small size, LOD score calculated separately for each of the two families did not reach a value greater than 3. Although locus heterogeneity cannot be absolutely ruled out, the very large size of the interval shared by family 2 patients and the fact that family 1 patients did not display homozygosity for any other chromosomal region when screened with markers encompassing the whole genome do not support this possibility.

The disease interval shared by the two families described in this study harbors 73 genes. Among these, *PPHLN1* was considered as a good candidate because periphilin 1 plays a role during the maturation of the cornified cell envelope, a major step during normal epidermal differentiation and barrier formation (Kazerounian and Aho, 2003). Periphilin 1 is found *in vitro* in the nucleus of undifferentiated keratinocytes but at the cell periphery in differentiated keratinocytes, colocalizing there with periplakin (Kazerounian and Aho, 2003). Alternative splicing of 5′-exons 2, 4, and 7 and 3′-exons 11–14, gives rise to multiple protein products. The exclusion of exon 2 deletes the first in-frame translation initiation codon. The second in-frame ATG encodes Met-8. No pathogenic mutations were, however, identified in all potential coding regions of the gene in our study. Other candidates present within the disease interval and deserving further scrutiny include *ADAMTS20*, a disintegrin-like metalloprotease (Somerville *et al*, 2003) and *TMEM16F*, a transmembrane protein (Katoh and Katoh, 2004), presenting structural but no sequence similarity to other transmembranal proteins previously found to be involved in the pathogenesis of CRI (Lefevre *et al*, 2004). ABCD2, also present within the disease interval, is a member of the ABC transporter family. Another member of this protein family has been implicated in the pathogenesis of CRI (Lefevre *et al*, 2003). ABCD2, however, is speculated to function as a dimerization partner of ABCD1 and other peroxisomal ABC transporters, and is thought to play a role in the pathogenesis of adrenoleukodystrophy (Liu *et al*, 1999). Expression and mutation analysis of these and other candidate genes within the disease interval as well as fur-

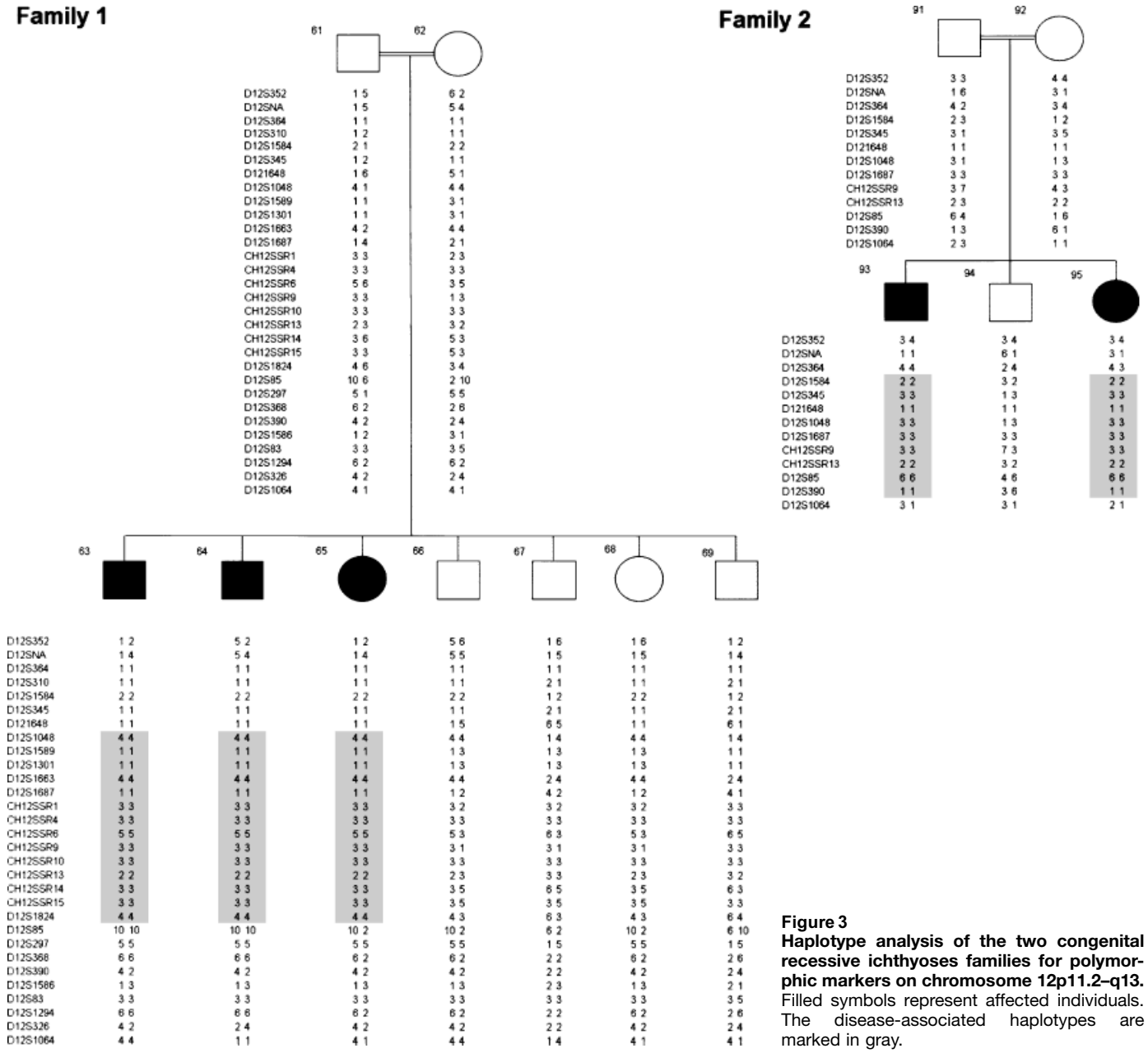

Figure 3
Haplotype analysis of the two congenital recessive ichthyoses families for polymorphic markers on chromosome 12p11.2–q13. Filled symbols represent affected individuals. The disease-associated haplotypes are marked in gray.

ther reduction of the disease interval through assessment of additional families should lead to the identification of a novel gene coding for a protein of importance in the maintenance of proper epidermal differentiation.

Materials and Methods

Patients and biological materials All participants or their legal guardians provided written and informed consent according to a protocol previously approved by the local Helsinki Committee and by the Committee for Genetic Studies of the Israeli Ministry of Health. Blood samples were drawn from all family members, and DNA was extracted according to standard procedures.

Genotyping Genomic DNA was PCR amplified using either fluorescently labeled primer pairs (Research Genetics, Invitrogen, Carlsbad, California) or non-labeled primer pairs encompassing 26 chromosomal microsatellite repeats (Table I).

PCR conditions were: 95°C for 4 min followed by 35 cycles at 95°C for 30 s, 55°C for 30 s (when not otherwise specified in Table I), 72°C for 30 s, and a final extension step at 72°C for 5 min. For semi-automated genotyping, PCR products were separated by PAGE on an ABI 310 sequencer system, and allele sizes were determined with Genescan 3.1 and Genotyper 2.0 software (PE Applied Biosystems, Foster City, California). For manual genotyping, amplicons were electrophoresed on 6% acrylamide gels followed by silver staining as previously described (Merril, 1986).

***PPHLN1* gene analysis** Genomic DNA was PCR amplified using primer pairs encompassing all exons and exon–intron boundaries of the *PPHLN1* gene (Table II). Cycling conditions were 95°C for 5 min followed by 35 cycles at 95°C for 30 s, 57°C–60°C for 45 s, 72°C for 90 s, and a final extension step at 72°C for 7 min. Resulting amplicons were gel-purified (QIAquick gel extraction kit, Qiagen, Valencia, California) and subjected to bi-directional DNA sequencing using the BigDye terminator system on an ABI Prism 3100 sequencer (PE Applied Biosystems).

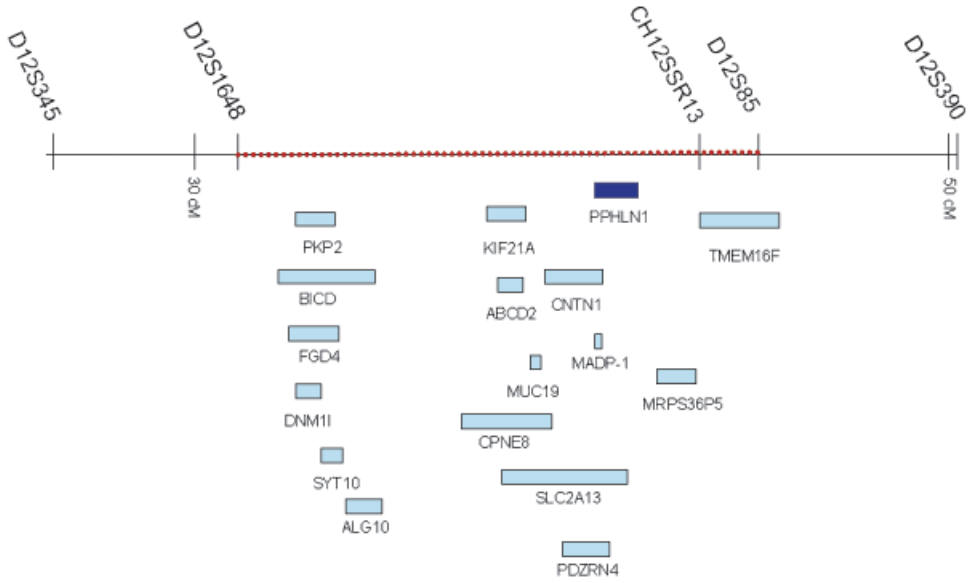

Figure 4
Chromosomal map of the new congenital recessive ichthyoses locus. The relative position of selected polymorphic markers and genes is shown according to Mapviewer. Distances in centiMorgan indicate distance from markers to the telomeric end of the chromosome p-arm. The disease interval defined by haplotype analysis is marked in red.

For RT-PCR, total RNA was extracted from a snap-frozen skin biopsy obtained from non-lesional skin using the RNeasy extraction kit (Qiagen) and amplified using the TITAN One Tube RT-PCR kit (Roche Molecular Biochemicals, Mannheim, Germany) and intron-crossing primer pairs specific for *PPHLN1* located in exon 3 and 5, respectively (forward 5′-CATTTAGCTCATTCGATTAAG-3′ and reverse 5′-CACATGAGAGCATCAAGCAG-3′). PCR conditions were: 30 min at 50°C; 94°C for 2 min; 94°C for 30 s, 60°C for 30 s, and 68°C for 90 s, for a total of 10 cycles; 94°C for 30 s, 60°C for 30 s, and 68°C for 90 s + 5 additional seconds at each cycle, for a total of 25 cycles; and final extension step at 68°C for 7 min. The resulting amplicons were then amplified using Taq polymerase, Q solution (Qiagen) and nested primers located in exons 3 and 5, respectively (forward 5′-GTGCTGGGATTACAGGCGTGAGTCAC-3′ and reverse 5′-GTGAACGAGCTCTACTGCAGGCTGCAG-3′). Cycling conditions were 95°C for 5 min followed by 35 cycles at 95°C for 30 s, 60°C for 45 s, 72°C for 90 s, and a final extension step at 72°C for 7 min. As a control, we amplified, as described above, total RNA with primers specific for β-actin (forward 5′-CCAAGGCCAACCGCGAGAAGATGAC-3′ and reverse 5′-AGGGTACATG GTGGTGCCGCCAGAC-3′).

Statistical analysis of linkage data Linkage analysis was performed using either the SuperLink package software (http://bioinfo.cs.technion.ac.il/superlink/) (Fishelson and Geiger, 2002) or the HOMOZ software (http://www.rfcgr.mrc.ac.uk/Registered/Option/homoz.html) (Kruglyak *et al*, 1995). The disease trait was modeled as autosomal recessive, fully penetrant, with no interference and with an allele frequency of 0.0001. Allele frequencies for all (known and newly developed) markers were calculated from a pool of 20 DNA samples obtained from population-matched unrelated healthy individuals.

We are grateful to the family members for their participation in our study. We wish to thank Dr Vered Friedman for services in nucleic acid analysis, and Ma'ayan Fishelson and Anna Tzemach for computer assistance. This study was supported in part by a grant provided by the Ruth and Allen Ziegler Fund for Pediatric Research.

Table II. Nucleotide sequences of primers used to amplify *PPHLN1*

Exon	Forward primer	Reverse primer	Product size (bp)
1	GGTTGGTTTATACAGACACAAATC	GTAACAATAACTACTATATTAAATAC	126
2	GTAATCATTTACTCCTTCCTTAC	CCTAGCTTTGGTGTATCAAATTAATTC	189
3	CAGTCAGTCTACTCTTTCAG	GACTATGTAGTATAATAGCAC	248
5	CAGTCAGTCTACTCTTTCAG	GTGCTATTATACTACATAGTC	404
6	GTGCTGGGATTACAGGCGTGAGTCAC	GTGAACGAGCTCTACTGCAGGCTGCAG	373
7	CTCATCACTCCTACTTCTGAG	CTACAGATCTCAGCCTCCTACAG	443
8	GGTTATTTCAGATTGTTGATGG	AGCATCTGTACTAGTCAGTC	391
9	GAATGTACCTGTTCTCCATAG	CATTCAGACAAAGCGTGATTACTG	256
10	GCCAGTTAGTGCCTATACAC	GATCAAACTGACTGTGAAGTC	391
11	GATGTCAGCATCATAATTCTGC	GAGTGGAAGTATCATACTCTGC	256
12	CAGCTTATCAGGACTGCACTCTC	CTGTTGTGTGGATAGCTGTTG	306
13	GATTCCAGCACGACGCATCA	AGTCACACTGCTAGACGCTG	431
14	CAGCGTCTAGCAGTGTGACT	CTGACCATCTCCTACATCAC	325

DOI: 10.1111/j.0022-202X.2005.23777.x

Manuscript received February 1, 2005; revised March 2, 2005; accepted for publication March 3, 2005

Address correspondence to: Eli Sprecher, MD, PhD, Laboratory of Molecular Dermatology, Department of Dermatology, Rambam Medical Center, Haifa, Israel. Email: e_sprecher@rambam.health.gov.il

References

Akiyama M, Sawamura D, Shimizu H: The clinical spectrum of nonbullous congenital ichthyosiform erythroderma and lamellar ichthyosis. Clin Exp Dermatol 28:235–240, 2003

Chavanas S, Bodemer C, Rochat A, *et al*: Mutations in SPINK5, encoding a serine protease inhibitor, cause Netherton syndrome. Nat Genet 25:141–142, 2000

De Laurenzi V, Rogers GR, Hamrock DJ, *et al*: Sjogren–Larson syndrome is caused by mutations in the fatty aldehyde dehydrogenase gene. Nat Genet 12:52–57, 1996

DiGiovanna JJ, Robinson-Bostom L: Ichthyosis: Etiology, diagnosis, and management. Am J Clin Dermatol 4:81–95, 2003

Fischer J, Faure A, Bouadjar B, *et al*: Two new loci for autosomal recessive ichthyosis on chromosome 3p21 and 19p12–q12 and evidence for further genetic heterogeneity. Am J Hum 66:904–913, 2000

Fishelson M, Geiger D: Exact genetic linkage computations for general pedigrees. Bioinformatics 18:S189–S198, 2002

Hatsell SJ, Stevens H, Jackson AP, Kelsell DP, Zvulunov A: An autosomal recessive exfoliative ichthyosis with linkage to chromosome 12q13. Br J Dermatol 149:174–180, 2003

Irvine AD, Paller AS: Molecular genetics of the inherited disorders of cornification: An update. Adv Dermatol 18:111–149, 2002

Ishida-Yamamoto A, Iizuka H: Structural organization of cornified cell envelopes and alterations in inherited skin disorders. Exp Dermatol 17:1–10, 2002

Jobard F, Lefevre C, Karaduman A, *et al*: Lipoxygenase-3 (ALOXE3) and 12(R)-lipoxygenase (ALOX12B) are mutated in non-bullous congenital ichthyosiform erythroderma (NCIE) linked to chromosome 17p13.1. Hum Mol Genet 11:107–113, 2002

Katoh M, Katoh M: Identification and characterization of TMEM16E and TMEM16F genes in silico. Int J Oncol 24:1345–1349, 2004

Kazerounian S, Aho S: Characterization of periphilin a wide-spread, highly insoluble nuclear protein and potential constituent of the keratinocyte cornified envelope. J Biol Chem 278:36707–36717, 2003

Krebsova A, Kuster W, Lestringant GG, *et al*: Identification, by homozygosity mapping, of a novel locus for autosomal recessive congenital ichthyosis on chromosome 17p, and evidence for further genetic heterogeneity. Am J Hum Genet 69:216–222, 2001

Kruglyak L, Daly MJ, Lander ES: Rapid multipoint linkage analysis of recessive traits in nuclear families, including homozygosity mapping. Am J Hum Genet 56:519–527, 1995

Laiho E, Ignatus J, Mikkola H, *et al*: Transglutaminase 1 mutations in autosomal recessive ichthyosis: Private and recurrent mutations in an isolated population. Am J Hum Genet 61:529–538, 1997

Lefevre C, Audebert S, Jobard F, *et al*: Mutations in the transporter ABCA12 are associated with lamellar ichthyosis type 2. Hum Mol Genet 12:2369–2378, 2003

Lefevre C, Bouadjar B, Karaduman A, *et al*: Mutations in ichthyin, a new gene on chromosome 5q33, in a new form of autosomal recessive congenital ichthyosis. Hum Mol Genet 13:2473–2482, 2004

Lefevre C, Jobard F, Caux F, *et al*: Mutations in CGI-58, the gene encoding a new protein of the esterase/lipase/thioesterase subfamily, in Chanarin–Dorfman syndrome. Am J Hum Genet 69:1002–1012, 2002

Liu LX, Janvier K, Berteaux-Lecellier V, Cartier N, Benarous R, Aubourg P: Homo- and heterodimerization of peroxisomal ATP-binding cassette half-transporters. J Biol Chem 274:32738–32743, 1999

Merril CR: Development and mechanisms of silver stains for electrophoresis. Acta Histochem 19:655–667, 1986

Russell LJ, DiGiovanna JJ, Rogers GR, *et al*: Mutations in the gene for transglutaminase 1 in autosomal recessive lamellar ichthyosis. Nat Genet 9: 279–283, 1995

Somerville RP, Longpre JM, Jungers KA, *et al*: Characterization of ADAMTS-9 and ADAMTS-20 as a distinct ADAMTS subfamily related to *Caenorhabditis elegans* GON-1. J Biol Chem 278:9503–9513, 2003

Virolainen E, Wessman M, Hovatta I, *et al*: Assignment of a novel locus for autosomal recessive congenital ichthyosis to chromosome 19p13.1–p13.2. Am J Hum Genet 66:1132–1137, 2000

Williams ML, Elias PM: Heterogeneity in autosomal recessive ichthyosis: Clinical and biochemical differentiation of lamellar ichthyosis and non-bullous congenital ichthyosiform erythroderma. Arch Derm 121:477–488, 1985

Zlotogora J: Autosomal recessive diseases among Palestinian Arabs. J Med Genet 34:765–766, 1997

Appendix: Electronic database information

The URLs for data presented herein are as follows:

HOMOZ software: http://www.rfcgr.mrc.ac.uk/Registered/Option/homoz.html
Superlink software: http://bioinfo.cs.technion.ac.il/superlink/
Mapviewer: http://www.ncbi.nlm.nih.gov/mapview/map_search.cgi?taxid=9606